An Energy Storage System Utilization for Performance Enhancement of Wind Catcher Cooling

Nekoonam, Saeed; Pourfayaz, Fathollah*[+]

Department of Renewable Energies and Environment, Faculty of New Sciences and Technologies, University of Tehran, Tehran, I.R. IRAN

ABSTRACT: *High peaks of electrical energy usage during hot days of summer, have become an issue for the power supply systems causing regional power outages. Cooling demand is the main reason for such energy load, which is majorly supplied by electricity. It is possible to use the night cold air for daytime cooling. Energy storage is necessary for the usage of this night-cold energy. The night ambient temperature is usually not cold enough to provide the required low-temperature heat transfer fluid flow and also the daytime cooling demand is usually high. A novel system where a storage unit is connected to a wind catcher has been investigated in this study. The results showed that this new system covers the above-mentioned problems. According to the final results, 12.8 kWh of cold energy was stored in the energy storage unit, presenting 64 % of energy storage efficiency and 6h 3m of the charging required time during the night. It was also revealed that the energy storage unit's thermal performance, is highly relevant to the inlet temperature, where 5 °C decreases in the inlet temperature, increased the stored energy by 17%, and decreased the charging required time by 1h 33m.*

KEYWORDS: *Thermal storage; Phase change; Wind catcher; Night cool.*

INTRODUCTION

The world`s energy demand is inevitably dependent on fossil fuel consumption. Therefore, more than 90 million barrels of oil are traded daily to supply the final energy and the required substances. This withdrawal of non-renewable energy sources has made it difficult for the environment to dissolve the released pollution. Therefore, greenhouse gases, climate change, the atmosphere, and the earth's pollution phenomena have resulted. An important reason for the energy usage is providing the thermal comfort of the living areas, heating for the winter, and cooling for the summer. One of the energy system problems during recent years is the high electrical energy peak load usage during hot days of the summer (as a result of the high solar solar radiation [1-3]), which causes power outages or shutdown of some industries by the governmental order. Unlike heating which can be provided by different energy carriers like natural gas [4], kerosene [5], and electricity [6], electricity is usually used by cooling systems. A typical cooling system consists of evaporative cooling [7] and air conditioners [8, 9]. In the case that a part of the required cooling power is supplied by a source other than electricity, some of the peak load is shaved.

A considerable temperature difference between the day and night is pretty usual in dry climates [10], it is also varied seasonably [11, 12]. Therefore, usage of the night cool air during the summer [13] can be considered an option.

***To whom correspondence should be addressed.*
+ E-mail: pourfayaz@ut.ac.ir
1021-9986/2022/6/2087-2099 13/$/6.03

The majority of the cooling load requirement occurs during the day [14]. Therefore, energy storage is required. Of all the different storage techniques, there are two major thermal storage methods: sensible and latent storage. Sensible energy storage has a relation with the temperature and is also related to the mass and the thermal capacity [15]. Latent energy storage involves phase change. Therefore, the stored energy does not have a linear relation with the temperature [16]. It is also known that more amount of energy is stored in the latent storage compared to the sensible storage with the same volume [17-19].

An ancient and common system which is called a wind catcher was used to provide the required cold energy in hot areas. In this technology, the wind is directed through the channels, which continue to 5 meters below the ground surface, reaching a depth where the temperature is almost fixed during the year and is usually about 20°C. The inlet airflow gets cold by losing its energy and is then prepared for thermal comfort utilization. During the night, the required cooling load is decreased. Therefore, a portion of the cold air which is provided by the wind catcher is used to charge the energy storage unit where the stored energy is used during the day. A heat transfer model for cooling buildings was developed by *Turnpenny et al.* [20], where the air is the Heat Transfer Fluid (HTF), and the system optimized dimensions were reported according to the demand. The developed system was designed so that the air is passed through the heat pipes which are connected to the Phase Change Material (PCM) [21]. The authors concluded that the temperature difference between the HTF and the PCM has a high effect on the thermal performance and efficiency of the system. *Hed* and *Bellander* [22] used the PCM for storing the night cool. The finite difference was used to develop the storage model and the authors also developed a unique heat transfer coefficient that seemed to match the shape of the investigated heat exchanger. According to the authors, variations in the heat capacity regarding the temperature has a considerable effect on the performance of the heat exchanger. The performance of the storage unit is related to the optimum amount of phase change material, which is placed inside the unit.

A lab-scale storage system with PCM was built and investigated by *Lazaro et al.* [23]. Night cool was stored in the system and it was discharged during the day. The authors' investigation showed that although the heat transfer through the PCM is low, with an appropriate system design, the system can provide acceptable cooling power and can be used for passive cooling. In another study, a system of PCMs was added to an air conditioning system by *Parameshwaran et al.* [24]. The new system was then investigated. The authors concluded that the thermal performance and the energy usage of the air conditioning system increased by 28 % and 47 % respectively based on the summer situation and the winter situation. *El Mankibi et al.* [25] investigated utilizing a verified numerical model which was developed based on the energy equations and the heat capacity method. The effect of different parameters such as unit dimensions, amount, and specification of the PCM on the optimized performance of the system was investigated. The developed model was connected to a building simulator. Different scenarios of thermal comfort and the inside air quality were included in the building model. The optimized dimensions, volume, type, and specification of the studied PCMs were reported by the authors.

The thermal behavior of a PCM-based flat plate latent heat storage unit was tested based on the analytical techniques by *Ding et al.* [26]. Analytical terms of the HTF temperature distribution were developed by the energy conservation equations solution and it was validated by the authors' experimental results. In another study, three different configurations of an energy storage unit were analyzed and compared for their thermal performance by *Xu et al.* [27]. According to the results, the slab capsule configuration shows the highest total capacity for energy storage (710 kWh) and also the charge situation (40%), when three hours of charging was applied to all cases, although this design has a low total storage capacity on theory (1760 kWh). For analyzing the thermal behavior of a PCM-based slab thermal energy storage unit under different situations, an experimental setup was made to examine the effect of the HTF temperature, HTF velocity, and plate inclination by *Sun et al.* [28]. According to the results, as the natural convection occurs within the PCM, the melting temperature margin differs under various conditions. It was important to define the melting temperature range which practically happens to receive the melting performance prediction accurately.

According to the research background, the PCM was used for cooling storage. However, because of the cool

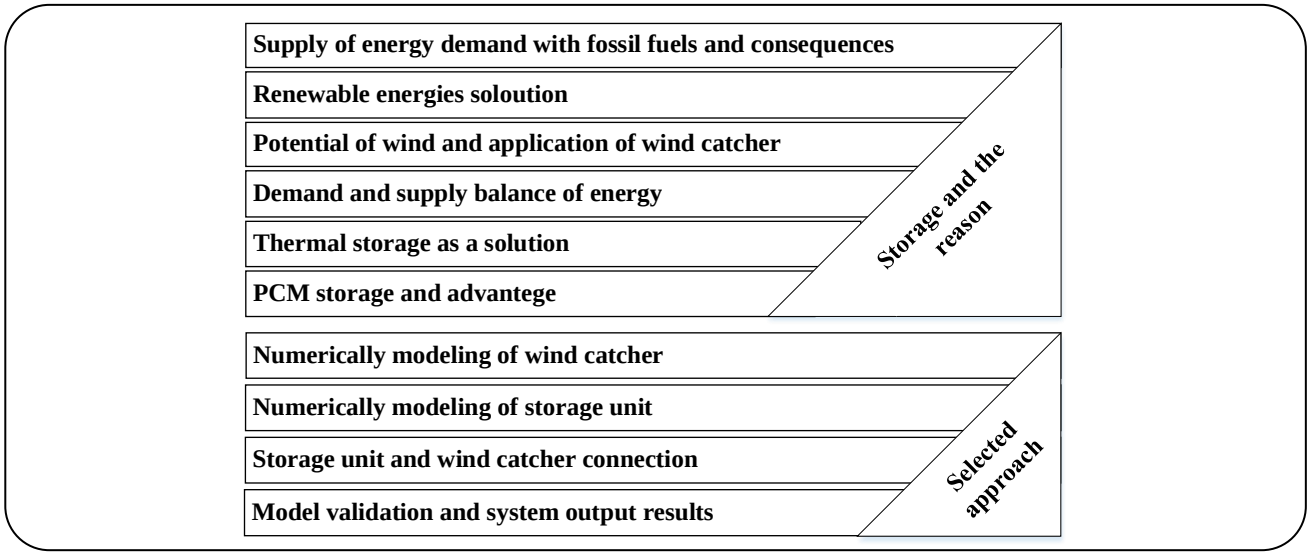

Fig. 1: Key reasons for the storage application and the problem-solving approach.

night air temperature margins which narrow the efficient application, this type of storage is very suitable for the areas where the temperature difference between the day and the night is high. On the other hand, wind catchers have also been used for cooling, but because of the limited air temperature margins they create; as the input air gets hotter during the day and the ambient temperature approaches the maximum, the performance of the wind catcher drops significantly.

In this study, researchers have proposed a system that provides both the low-temperature required cooling air for the storage, and by using the storage system, the performance of the wind catcher system during mid-day high ambient temperature hours was increased. In this investigation, a storage unit with the PCM was modeled and utilized for storing the night cool. The storage unit was connected to a wind catcher which provides the required cool air. The storage unit was modeled utilizing the thermal governing equations and it was validated with the experimental data of the literature. RT 21 was used as the PCM. For analyzing the cooling performance of the system, the hottest day of the summer was selected. Night air enters the storage unit after passing through underground channels of the wind catcher and it releases the energy to the PCM to charge the storage unit at night, then the energy storage unit is discharged to cool up the target area during the day.

EXPERIMENTAL SECTION

Different parts of the system containing the storage unit and the wind catcher are introduced in this section and the connection between them is defined. The problem-solving approach and the necessity of energy storage are also defined in Fig. 1.

System structure

The investigated system consisted of a wind catcher and an energy storage unit, where air enters the wind catcher during the night and passes through the underground channels, a portion of the cooling airflow goes to direct usage and the rest goes to charge the energy storage unit. During the day, the required cooling power is increased. Therefore, the wind catcher outlet flow goes totally to the direct usage, and the storage unit is also discharged. The overall system is depicted in Fig. 2.

Storage unit

Aluminum slab plates are filled with the PCM which acts as a heat exchanger and absorbs energy from the passing air and stores it. The plates of the storage unit are as depicted in Fig. 3b. There are 100 slab plates inside the energy storage unit, which are arranged as depicted in Fig. 3a. The plates are arranged in 5 columns and 20 rows. The flow of the HTF within the energy storage unit follows symmetry in the unit`s width and length direction.

PCMs have a high latent heat of phase change and a temperature interval at which the phase change process occurs. The thermal behavior of the PCMs is the same as sensible storage before and after the phase change, but during the phase change, a large amount of energy is stored

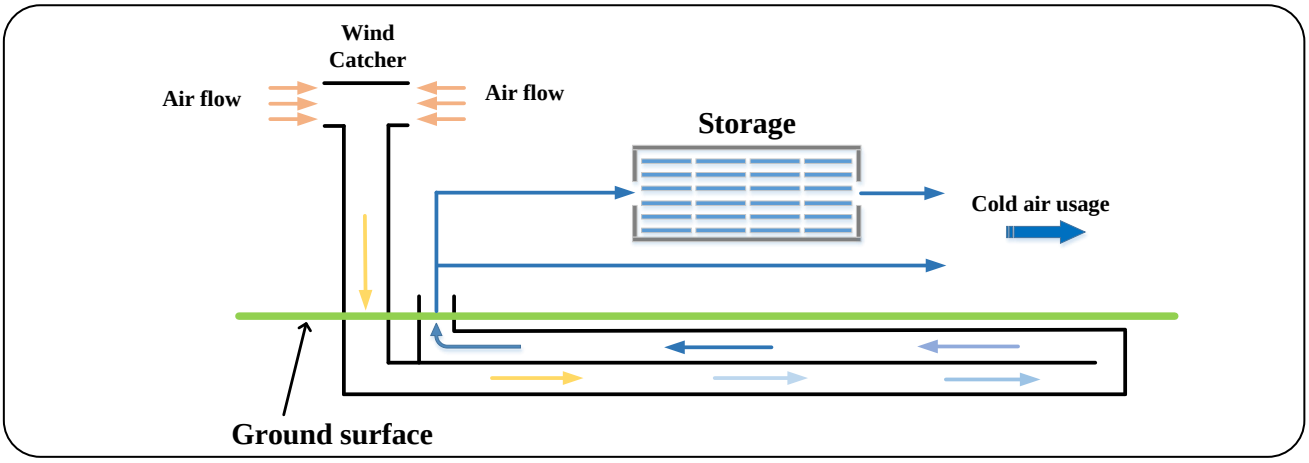

Fig. 2: Conceptual model of the investigated system.

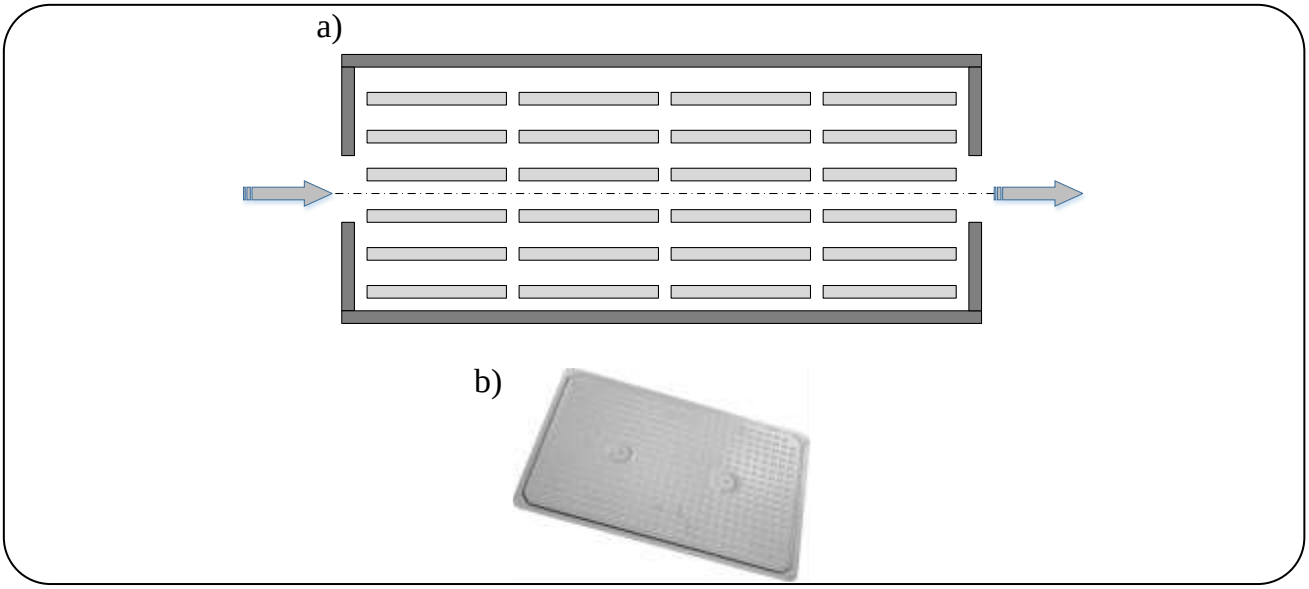

Fig. 3: a) The storage unit and the HTF flow b) PCM containing Plates [29].

in the PCM within the specific temperature interval. The latent heat and the phase change temperature of the PCM are the most important characteristics of this kind of material. Different types of PCMs are presented in Fig. 4, where these materials are categorized based on their structural components.

RT-type PCMs are common commercial paraffin-based PCM types, which are variously used for research and investigation cases. The manufacturer provides a detailed specification list for each PCM type, presenting various required characteristics of the material. In this research, RT 21 (which is of the paraffin-based organic PCM types, and is commercially available) is used as the PCM. The number in front of the "RT" is the phase change temperature. A complete specification list of the RT 21 is presented in Table 1. The paraffin-based PCMs are proper media for household energy storage applications, regarding the literature review [30]. According to the phase change temperature interval of the PCM and the proper latent heat capacity, it is understood that the selected PCM is a perfect match for the required application. It is also important to say this research focuses on the macro capsulated PCM other than the Nano PCM [31] situations.

Specifications of the energy storage unit, including slab plate dimensions, air channel height between the slabs, numbers of the columns and rows, and the HTF (air) flow rate, which is equal to 300 m^3/h were tabulated as Table 2.

Table 1: Specification of the PCM [32].

material	Phase change domain (°C)	Heat storage capacity within phase change (kJ/kg)	Solid and liquid heat capacity (kJ/kg.k)	c_m (kJ/kg.k)	T_m (°C)
RT 21	20-23	190	2	47.8	35

Table 2. Specification of the storage unit and the air:

Parameter	amount
Slab width, mm	300
Slab length, mm	450
Air channel`s height, mm	20
Columns No.	5
Rows No.	20
HTF flowrate, $m^3 h^{-1}$	300

Phase Change Materials

Organic

Paraffin

PCM	T_m [C]
$C_{18}H_{38}$	28
$C_{19}H_{40}$	32
$C_{20}H_{42}$	37
$C_{21}H_{44}$	41
$C_{22}H_{46}$	44
$C_{23}H_{48}$	47
$C_{24}H_{50}$	51
$C_{25}H_{52}$	54
$C_{26}H_{54}$	56
$C_{27}H_{56}$	59

Non-paraffin

PCM	T_m [C]
Capric Acid	28
Lauric Acid	42-44
Erythritol	118
Myristic Acid	49-51

Inorganic

Hydrate

PCM	T_m [C]
$CaCL_2$ $6H_2O$	29-30
CH_3COO $Na.3H_2O$	58
$MgCL_2$ $6H_2O$	115-117

Molten salt

PCM	T_m [C]
$NaNO_2$	282
$NaNO_3$	307
NaOH	318
LiOH	462
NaCl	800

Metallic

PCM	T_m [C]
Cu	1084
Al-Si	587

Eutectic

Organic-Organic

PCM	T_m [C]
Lauric-Capric acid (35-65 mol%)	18

Organic-Inorganic

PCM	T_m [C]
$NaNO_3$-KNO_3 (50-50 mol%)	220

Inorganic-Inorganic

PCM	T_m [C]
NH_2CONH_2 NH_4NO_3	46

Fig. 4: PCMs different types and their phase change temperature.

Windcatcher

Wind catchers (see Fig. 5) are structures that divert the passing wind around them through entrance windows to a target space, using passing channels. Usage of the wind catchers has been very common through the years in the central and southern cities of Iran [33]. The wind catchers are divided into two types, in the first type the air is cooled with the convection mechanism only, and in the second type, the air is cooled with convection and evaporation mechanisms simultaneously. In this investigated system, the ambient airflow is entered the wind catcher and is delivered to the target space by losing temperature and by passing the channels, which are made of brick and are located approximately 5 m under the ground surface. According to Fig. 5, wind catchers have majorly consisted of a heading part, a channel part, and a roof. The parts are shown in Fig. 5 and the structure is placed on the roof of a building in order to receive the most possible airflow.

According to the system, the wind is entered into the wind catcher and goes through the underground channels. The annual temperature distribution of Tehran is depicted in Fig. 6. Based on the figure, the highest temperature was reached annually equal to 41 °C and the lowest was -8.1 °C. The meteorology data which is depicted in Fig. 6 was analyzed as hourly sets of temperatures, such as the input temperature of the wind catcher case.

Table 3: Hourly temperature distribution of the hottest day of the year.

Hour	0	1	2	3	4	5	6	7	8	9	10	11
Temperature	30.5	30.6	30.8	31	32.8	35.6	37.2	37.7	38.2	38.8	39.5	40.2
Hour	12	13	14	15	16	17	18	19	20	21	22	23
Temperature	41	40.6	40.2	39.8	39.8	37	35.5	34.8	34.1	33.5	32.7	31.5

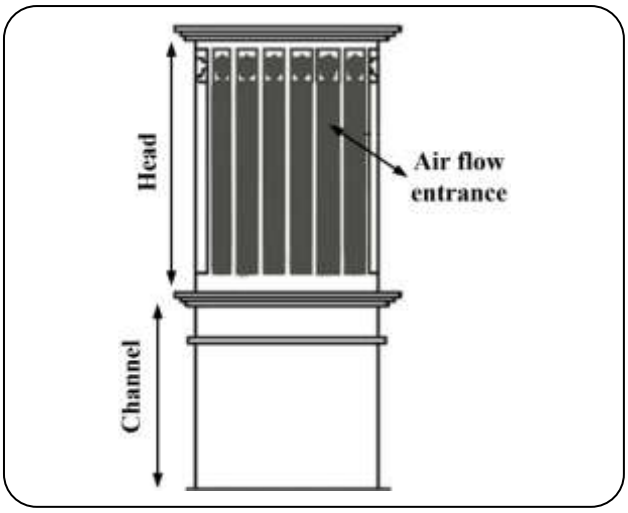

Fig. 5: The wind catcher heading parts.

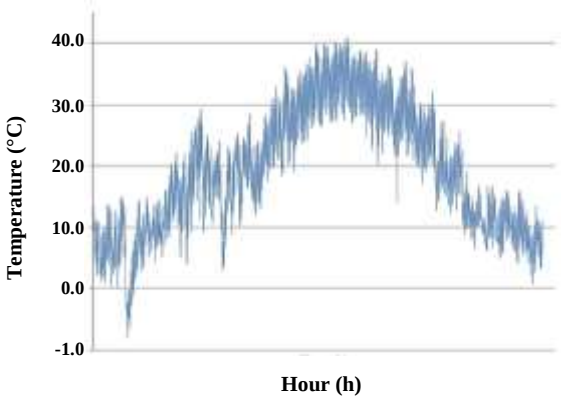

Fig. 6: The annual temperature distribution of Tehran, the high amounts presenting the summer period and the low amounts for the winter.

Tehran is the capital and largest city of the country, and the highest amount of energy is consumed in this city. Therefore, the city was selected for the investigation. The hottest day of the summer (26th of July) was selected for analyzing the system performance. The temperature distribution of the selected day is tabulated in Table 3.

System modeling

The following assumptions were made for preparing the governing equations of the system:

(1) Fluid flow inside the energy storage unit is fully developed and laminar.

(2) Material specifications are fixed and the temperature variations have no effect on the thermal characteristics.

(3) Heat loss from the storage unit walls, is considered to be a maximum 5% (based on the input energy).

(4) The aluminum slabs are the same size and contained the same amount of the PCM.

(5) Temperature distribution of the unit is in two directions and the heat transfer parallel to the slab length is considered to be negligible.

According to the energy balance [34], the energy equation of the fluid was developed as Equation (1):

$$h(m.\Delta x).(T_s - T_a) + \rho_a.v\left(\frac{L}{2}.m\right)(h_x - h_{x+\Delta x}) = \rho_a.c_a.\left(\frac{L}{2}.m.\Delta x\right).\frac{\partial T_a}{\partial t} \quad (1)$$

h is the conductive heat transfer coefficient of the fluid, m is the thickness of the element, Δx is the spatial horizontal step, T_s is the PCM container`s surface temperature, T_a is the fluid temperature, ρ_a is the fluid density, v is the fluid velocity, L is the normal distance between the two slabs of the storage unit, h_x is the fluid enthalpy at the element entrance, $h_{x+\Delta x}$ is the fluid enthalpy at the element outlet and C_a is the fluid thermal capacity and t is the time. Equation 2 is generated by simplification of Equation (1):

$$v.\frac{\partial T_a}{\partial x} + \frac{\partial T_a}{\partial t} = \frac{2h}{\rho_a.L.c_a}.(T_s - T_a) \quad (2)$$

Equation (3) is formed by the energy balance [34] of the slab element.

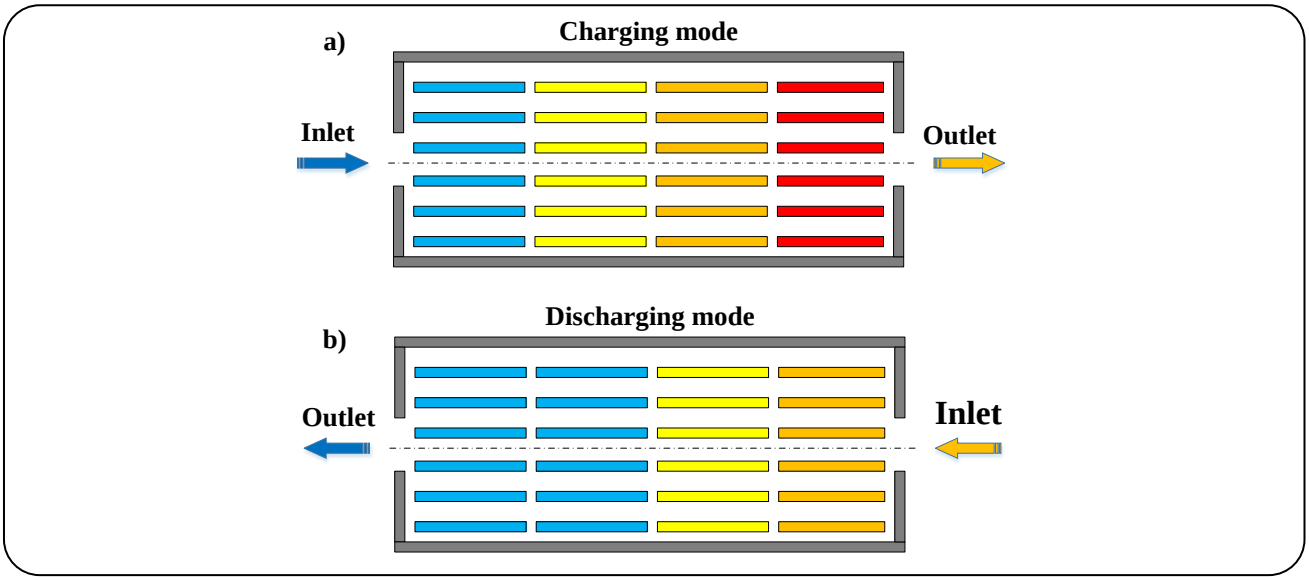

Fig. 7: a) The storage unit charging with the wind catcher outlet air b) the storage unit discharging to target space.

$$k_s.\Delta x.m.\left(\frac{\partial T_s}{\partial y}\right)_1 + k_s.\Delta x.m.\left(\frac{\partial T_s}{\partial y}\right)_2 = \rho_s.c_s.\Delta x.\Delta y.m.\left(\frac{\partial T_s}{\partial t}\right) \quad (3)$$

K_s is the container`s thermal conductivity coefficient, Δy is the vertical spatial step, T_s is the slab temperature, ρ_s and C_s are the density and the thermal capacity of the slab respectively, Equation (3) is simplified to Equation (4):

$$k_s.(\frac{\partial T_s}{\partial y})_1 + k_s.(\frac{\partial T_s}{\partial y})_2 = \rho_s.c_s.\Delta y.(\frac{\partial T_s}{\partial t}) \quad (4)$$

Equation (5) is formed by the energy balance at the PCM element:

$$k_p.\Delta x.m.\left(\frac{\partial T_p}{\partial y}\right)_1 + k_p.\Delta x.m.\left(\frac{\partial T_p}{\partial y}\right)_2 = \rho_p.c_p.\Delta x.\Delta y.m.\left(\frac{\partial T_p}{\partial t}\right) \quad (5)$$

Where K_p is the PCM`s heat transfer coefficient, Δy is the vertical spatial step, T_p is the PCM temperature, and ρ_p and C_p are the density and the thermal capacity of the PCM. The simplified form of Equation (5) is presented as Equation (6):

$$k_p.\left(\frac{\partial T_p}{\partial y}\right)_1 + k_p.\left(\frac{\partial T_p}{\partial y}\right)_2 = \rho_p.c_p.\Delta y.\left(\frac{\partial T_p}{\partial t}\right) \quad (6)$$

Effective thermal capacity [35] is a fast and precise form of the PCM numerical computing method. The latent heat of the phase change is equalized to an amount of thermal heat capacity, the method is called apparent heat capacity [36] which is numerically presented as Equation (7).

The thermal behavior of the energy storage unit in charging and discharging modes is presented in Fig. 7. The overall temperature of the unit (which was initially high) is lowered during the charge, and a reverse process has occurred during the discharge.

$$c_{eff}(t) = c + c_m.\exp\left\{-\frac{(t-t_m)^2}{2.1}\right\} \quad (7)$$

c_{eff} is the effective thermal capacity, c is the average thermal capacity of the PCM within the solid and liquid phase, c_m is the maximum thermal capacity regarding to the phase change, t is the PCM temperature and t_m is the average phase change temperature of the PCM [37].

Initial and boundary conditions of the system are explained as follows. Equation (8) indicates the initial condition of the PCM and Equation (9) indicates the initial condition of the solid surface. Equation (10) shows the initial condition of the input air as the HTF, where it is the same as the ambient temperature at the start. Equation (11) indicates the boundary condition of the air at the unit entrance and Equation (12) indicates the boundary condition of the air at the output.

$$T_p(x, y, t=0) = T_0 \quad (8)$$

$$T_s(x, y, t=0) = T_0 \quad (9)$$

$$T_a\left(x, y, t=0\right)=T_{amb} \quad (10)$$

$$T_a\left(x=0, t\right)=T_{in} \quad (11)$$

$$T_p\left(x=x_{end}, t\right)=T_{out} \quad (12)$$

In order to solve the equations and receive the temperature distribution within the energy storage unit and the stored energy calculation, MATLAB software was utilized.

Mesh independency investigation

The solution process of the numerical model is needed to be independent of the time and the spatial steps, also in order to optimize the computational costs, mesh dimensions are needed to have an optimal amount. Therefore, time and spatial steps were investigated for optimum results.

The model results for the 2nd minute of running are illustrated in Fig. 8 and three-time steps of 0.05, 0.01, and 0.001 seconds were investigated. 2 % of the difference in the results was obtained from the 0.05 and 0.01-time steps. Therefore, 0.01 and 0.001-time steps were investigated and less than 1 % of the difference in the results was reported. As a result, 0.01 (s) was selected as the optimal time step of the numerical model and the 0.001 (s) time step was neglected because of the unnecessary high computational cost.

Three values of 10, 1, and 0.1 mm were tested as the possible optimal Δx values. Fig. 9 shows that comparing the results of the 10 and 1 mm steps have 3% difference and therefore the horizontal step needed to be reconsidered. Comparing the results of the 1 and 0.1 mm steps showed around 1% difference so the difference was negligible and 1 mm step was selected as the horizontal step.

According to Fig.10, there is around 3% difference in result cases of the 0.1 and 0.01 mm vertical spatial step, which means that smaller steps are needed to be applied. Therefore, 0.001 mm step was selected and the comparison of the results with the 0.01 mm step showed a lower than 1% of a difference the spatial step of 0.01 mm was then selected as the vertical step.

RESULTS AND DISCUSSION

Model verification

For verifying the developed model of the energy storage unit, model outputs were compared with the experimental results of *Charvat et al.* [38]. In order to do the verification, all the model inputs, such as dimensions

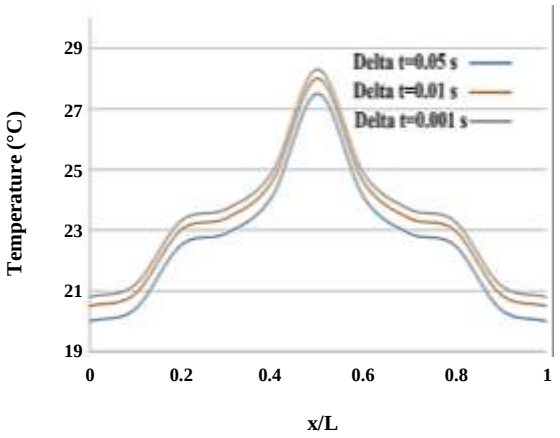

Fig. 8: Different time step results on the numerical solution in the 2nd minute of the computational run.

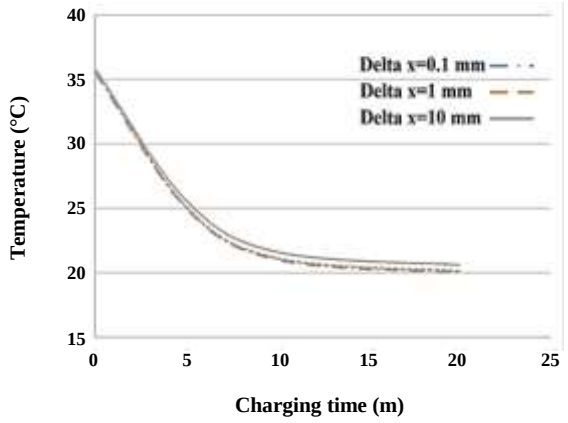

Fig. 9: Horizontal mesh independency evaluation at the outlet point of the single row till 20 m of charging.

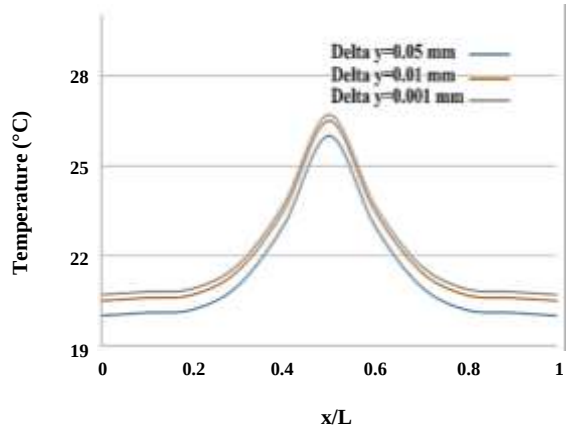

Fig. 10: The vertical mesh independency check at the t=4 min of charging.

Table 4. The hourly inlet and outlet temperatures of the wind catcher during the selected summer day.

Hour	Inlet temperature, °C	Outlet temperature, °C	Hour	Inlet temperature, °C	Outlet temperature, °C
0	30.5	20	12	41.0	27
1	30.6	20	13	40.6	26.6
2	30.8	20	14	40.2	26.2
3	31.0	20	15	39.8	25.8
4	32.8	20	16	38.4	24.4
5	35.2	21.2	17	37	23
6	37.2	23.2	18	35.5	21.5
7	37.7	23.7	19	34.8	20.8
8	38.2	24.2	20	34.1	20.1
9	38.8	24.8	21	33.5	20
10	39.5	25.5	22	32.7	20
11	40.2	26.2	23	31.5	20

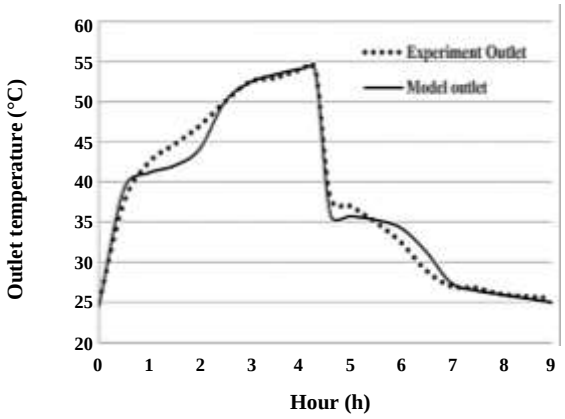

Fig. 11: Model validation with the experimental data of Charvat et al.

and specifications were applied completely the same as in the experimental situation. The model results and the experimental data showed a good match according to Fig. 11.

Performance of the system

According to Table 4, the wind catcher is providing a low-temperature air flow (20 °C) from 21:00 at night till 4:00 in the morning. This period of time which is literally 7 hours, is enough to completely charge the energy storage unit. Within this time, the cold air is inserted into the energy storage unit and the unit gets cooled up.

As it is presented in Table 4, the outlet temperature of the wind catcher is increased as the ambient temperature arises during the day. Owing to the variations in the humidity and cooling habits, recommendations for the summer and the winter temperature of the comfort zone may vary; a suggested typical range for the summer is approximately 23–25.5 °C. Based on this comfort temperature range, the energy storage system is performed the discharge process from 10:00 am (when the outlet temperature of the wind catcher reaches the higher limit of the comfort temperature) to 17:00 afternoon (when the outlet temperature of the wind catcher reaches the lower limit of the comfort temperature). After 17:00 in the afternoon, the outlet temperature of the wind catcher falls below 23 °C, in such case, the system could be turned off or continue working as the option of the user.

According to Fig. 12, the outlet temperature of the 4 different channels of the storage unit during the charge is reported. As it is presented, the 1st channel which is in the middle part of the energy storage unit and faces the highest air flow rate, is charged within 3 hours and the 7th channel which faces a low airflow the rate takes more than 5 hours to charge completely. This is presenting the reason why the overall energy storage unit

takes more than 5 hours to charge. The rows close to the wall which face a low HTF flow rate, increase the charging required time.

According to Fig. 13, 12.8 kWh of cold energy was stored in the energy storage unit (T_{in}=15 °C) when it was charged completely. The charging rate of the unit gets slower as more energy is stored. It is because of a decreasing temperature difference between the HTF and the PCM slabs, where this temperature difference is a critical factor in the heat transfer rate.

Two theoretical scenarios were also investigated in which, the inlet temperatures of the energy storage were lowered in order to analyze the effect of the inlet temperature on the performance of the energy storage unit. In the first case, the inlet temperature is put equal to 15 °C and as the results showed (See Fig. 13), more amount of energy was gained in the energy storage unit in a lower period (approximately 2 hours) and the final amount of the stored energy was also higher than the 20 °C cases, while it took less than 5 hours for the energy storage unit to get completely charged. The second analysis consisted of the inlet temperature equal to 10 °C and as the results show, the energy storage unit was charged by less than 4 h by storing a high amount of energy simultaneously. This is because of a high-temperature gradient value between the HTF and the phase change temperature of the PCM and as a result, the required charging time of the energy storage unit was shortened.

Fig. 14 shows the outlet temperature of the energy storage unit for different HTF input temperature cases. As the results show, the lower the input HTF temperature, the quicker the energy storage unit was charged and the shorter phase change process is gained.

Table 5 presents the performance situation of the studied case, where 12.8 kWh of stored energy and 64% of storage efficiency were obtained by the energy storage unit.

CONCLUSION

In this research, a wind catcher cooling system in connection with a PCM-based storage unit was investigated. A numerical thermal model was developed for the energy storage unit and the model was validated with the experimental data from the literature. The developed model accurately predicted the performance of the system with low computational cost because of the accurate mesh independency previous check.

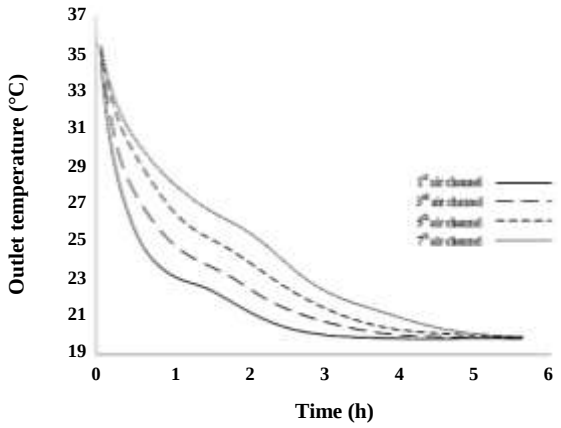

Fig. 12: Temperature distribution of the 4 different storage unit channels at the outlet point.

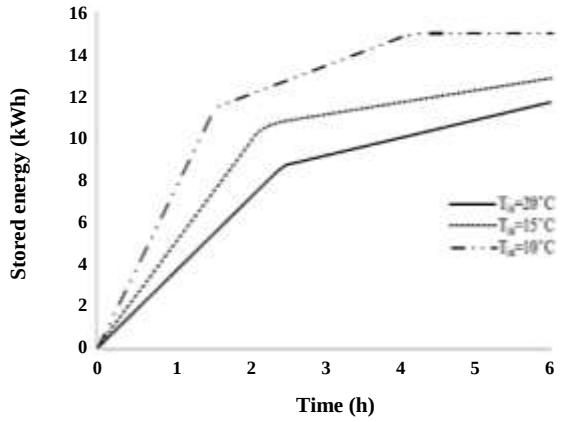

Fig. 13: Stored energy of the heat storage unit considering different inlet temperatures.

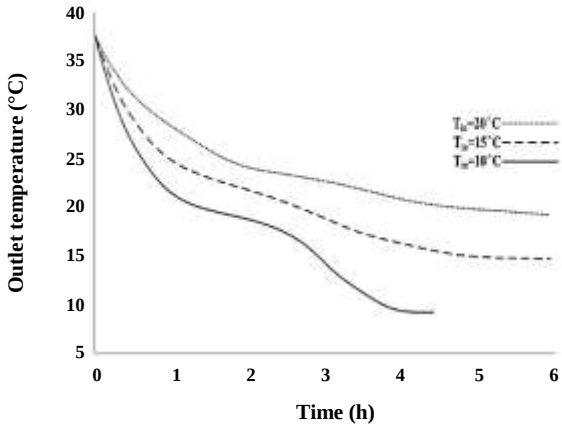

Fig. 14: The outlet temperature of the energy storage unit for the different HTF input temperature cases.

Table 5: The storage unit`s input and stored energy and the related efficiency.

PCM material	Inserted energy (kWh)	Stored energy (kWh)	Storage efficiency (%)
RT 21	20	12.8	64

The main findings of the current research are presented as follows:

(1) The PCMs are compatible with cold storage and are effectively applied in connection with the wind catcher system.

(2) Output temperature results from the different storage unit channels showed that the PCM in the first channel was fully charged within 3.3 hours and for the 3rd, 5th, and 7th channels, 4.2, 4.8, and 5.3 hours were needed to charge, respectively.

(3) Results showed that the effect of the inlet temperature on the charging time of the storage unit is very significant. 5 °C decrease in the inlet temperature reduces the charging required time by 1h 30m and 5 °C increase in the inlet temperature increases the charging required time by 50m.

(4) According to the results, the inlet temperature has a considerably high effect on the amount of stored energy. 5 °C Decrease in the inlet temperature increased the stored energy by 17%, while 5°C increase in the inlet temperature reduced this energy by 7%. The reason that the lower inlet temperature presents a greater effect on the stored energy amount, is the higher temperature gradient between the HTF and the PCM. Therefore, a higher heat transfer rate between the HTF and the PCM was obtained.

(5) The case study presented 12.8 kWh of stored energy and 64% of the storage efficiency during the 6h 3m of charging period.

It is recommended for future works to check the possibility and thermal efficiency of the system for possible application in the summer and winter for cold and hot storage by the same storage design. Also, financial analysis is recommended in order to find the best performance point of the system considering the financial cost.

Nomenclature

C	Heat capacity, kJ/kg K
C_{eff}	Effective heat capacity of PCM, kJ/kg K
C_m	PCM maximum heat capacity regarding phase change, kJ/kg K
h	Convective heat transfer coefficient, W/m^2 K
K	Thermal conductivity coefficient, W/m K
L	The vertical distance between two slabs, m
m	Surface unit area normal to the paper, m^2
T	Temperature, °C
T_m	Average phase change temperature of PCM, °C
T_0	Initial temperature, °C
v	Fluid velocity, m/s
Δx	Horizontal spatial step parallel to flow, m
Δy	Vertical spatial step, m

Subscripts

a	Fluid, air
end	Final mesh point
in	Input
out	Output
p	PCM
s	Surface (of PCM container)
x	Element inlet point
x+Δx	Element outlet point

Greek symbols

ρ	Density, kg / m^3

Abbreviations

HTF	Heat transfer fluid
PCM	Phase change material

Received :Oct. 25, 2021 ; Accepted : Jan. 31, 2022

REFERENCES

[1] Gilani H.A., Hoseinzadeh S., Techno-Economic Study of Compound Parabolic Collector in Solar Water Heating System In The Northern Hemisphere, *Applied Thermal Engineering*, **190**: 116756 (2021).

[2] Sohani A., Hoseinzadeh S., Berenjkar K., Experimental Analysis of Innovative Designs for Solar Still Desalination Technologies; an In-Depth Technical and Economic Assessment, *Journal of Energy Storage*, **33**: 101862 (2021).

[3] Pourmoghadam P., Farighi M., Pourfayaz F., Kasaeian A., Annual Transient Analysis of Energetic, Exergetic, and Economic Performances of Solar Cascade Organic Rankine Cycles Integrated with PCM-Based Thermal Energy Storage Systems, *Case Studies in Thermal Engineering*, **28**: 101388 (2021).

[4] Zhao N., Zhang Y., Li B., Hao J., Chen D., Zhou Y., Dong R., Natural Gas and Electricity: Two Perspective Technologies of Substituting Coal-Burning Stoves for Rural Heating and Cooking in Hebei Province of China, *Energy Science & Engineering*, **7(1)**: 120-131 (2019).

[5] Endale, A., Analysis of Status, Potential and Economic Significance of Solar Water Heating System In Ethiopia, *Renewable Energy*, **132**: 1167-1176 (2019).

[6] Kozarcanin, S., Andresen G., Staffell I., Estimating Country-Specific Space Heating Threshold Temperatures from National Gas and Electricity Consumption Data, *Energy and Buildings*, **199**: 368-380 (2019).

[7] Doğramacı P.A., Riffat S., Gan G., Aydın D., Experimental Study of the Potential of Eucalyptus Fibres for Evaporative Cooling, *Renewable Energy*, **131**: 250-260 (2019).

[8] Zheng L., Zhang W., Xie L., Wang W., Tian H., Chen M., Experimental Study on the Thermal Performance of Solar Air Conditioning System with MEPCM Cooling Storage, *International Journal of Low-Carbon Technologies*, **14(1)**: 83-88 (2019).

[9] Mohammadi K., McGowan J.G., A Thermo-Economic Analysis of a Combined Cooling System for Air Conditioning and Low to Medium Temperature Refrigeration, *Journal of Cleaner Production*, **206**: 580-597 (2019).

[10] Rahimi M., Hejabi S., Spatial and Temporal Analysis of Trends In Extreme Temperature Indices in Iran over the Period 1960–2014, *International Journal of Climatology*, **38(1)**: 272-282 (2018).

[11] Hoseinzadeh S., Ghasemi M.H., Heyns S., Application of Hybrid Systems in Solution of Low Power Generation at Hot Seasons for Micro Hydro Systems, *Renewable Energy*, **160**: 323-332 (2020).

[12] Hoseinzadeh S., Thermal Performance of Electrochromic Smart Window with Nanocomposite Structure under Different Climates in Iran, *Micro and Nanosystems*, **11(2)**: 154-164 (2019).

[13] Ji W., Wang H., Du T., Zhang Z., Parametric Study on a Wall-Mounted Attached Ventilation System for Night Cooling with Different Supply Air Conditions, *Renewable Energy*, (2019).

14] Fan C., Ding Y., Cooling Load Prediction and Optimal Operation of HVAC Systems Using a Multiple Nonlinear Regression Model, *Energy and Buildings*, **197**: 7-17 (2019).

[15] Cabeza L.F., Sensible Thermal Energy Storage at High Temperatures, in Recent Advancements in Materials and Systems for Thermal Energy Storage, Springer. p. 3-7 (2019).

[16] Nekoonam S., Roshandel R., Modeling and Optimization of a Multiple (Cascading) Phase Change Material Solar Storage System, *Thermal Science and Engineering Progress*, **23**: 100873 (2021).

[17] Babapoor A., Haghighi A.R., Jokar S.M., Ahmadi Mezjin M., The Performance Enhancement of Paraffin as a PCM During the Solidification Process: Utilization of Graphene and Metal Oxide Nanoparticles, *Iranian Journal of Chemistry and Chemical Engineering (IJCCE)*, **41(1)**: 37-48 (2020).

[18] Ahmadi Mezjin M., Karimi G., Medi B., Babapoor A., Paar M., Passive Thermal Management of a Lithium-Ion Battery Using Carbon Fiber Loaded Phase Change Material: Comparison and Optimization, *Iranian Journal of Chemistry and Chemical Engineering (IJCCE)*, **41(1)**: 310-327 (2020).

[19] Hussien S.A.H., Ali T. E, Abdel-Kariem S.M., Synthesis, DFT Calculations to investigate the Structure Electronic, Absorption Electronic Spectra, Antimicrobial Activity Application, and Non-Linear Optical Analysis of Pyridinyl and Pyrimidinyl Phosphonates Schemes, *Iranian Journal of Chemistry and Chemical Engineering (IJCCE)*, (2021).

[20] Turnpenny J., Etheridge D., Reay D., Novel Ventilation Cooling System for Reducing Air Conditioning in Buildings.: Part I: Testing and Theoretical Modelling, *Applied Thermal Engineering*, **20(11)**: 1019-1037 (2000).

[21] Nekoonam S., Ghasempour R., Optimization of a Solar Cascaded Phase Change Slab-Plate Heat Exchanger Thermal Storage System, *Journal of Energy Storage*, **34**: 102005 (2021).

[22] Hed G., Bellander R., Mathematical Modelling of PCM Air Heat Exchanger, *Energy and Buildings*, **38(2)**: 82-89 (2006).

[23] Lazaro A., Dolado P., Marín J.M., Zalba B., PCM–Air Heat Exchangers for Free-Cooling Applications in Buildings: Experimental Results of Two Real-Scale Prototypes, *Energy Conversion and Management*, **50(3)**: 439-443 (2009).

[24] Parameshwaran R., Harikrishnan S., Kalaiselvam S., Energy Efficient PCM-Based Variable Air Volume Air Conditioning System for Modern Buildings, Energy and Buildings, **42(8)**: 1353-1360 (2010).

[25] El Mankibi M., Stathopoulos N., Rezai N., Zoubir A., Optimization of an Air-PCM Heat Exchanger and Elaboration of Peak Power Reduction Strategies, *Energy and Buildings*, **106**: 74-86 (2015).

[26] Ding C., Niu Z., Li B., Hong D., Zhang Z., Yu M., Analytical Modeling and Thermal Performance Analysis of a Flat Plate Latent Heat Storage Unit, *Applied Thermal Engineering*, **179**: 115722 (2020).

[27] Xu T., Gkoutzamanis V.G., Dong H., Muhammad Y., Efstathiadis T.G., Kalfas A.I., Laumert B., Chiu J.N., Performance Evaluation of Three Latent Heat Storage Designs for Cogeneration Applications, *Solar Energy*, **225**: 444-462 (2021).

[28] Sun X., Mo Y., Li J., Chu Y., Liu L., Liao S., Study on the Energy Charging Process of a Plate-Type Latent Heat Thermal Energy Storage Unit and Optimization Using Taguchi Method, *Applied Thermal Engineering*, **164**: 114528 (20200.

[29] Dolado P., Lazaro A., Marin J.M., Zalba B., Characterization of Melting and Solidification in a Real Scale PCM-Air Heat Exchanger: Numerical Model and Experimental Validation, *Energy Conversion and Managemen*t, **52(4)**: 1890-1907 (2011).

[30] Kasaeian A., Pourfayaz F., Khodabandeh E., Yan W.M., Experimental Studies on the Applications of PCMs and Nano-PCMs in Buildings: A Critical Review, *Energy and Buildings*, **154**: 96-112 (2017).

[31] Abdoos B., Ghazvini M., Pourfayaz F., Ahmadi M.H., Nouralishahi A., A Comprehensive Review of Nano-Phase Change Materials with a Focus on the Effects of Influential Factors, *Environmental Progress & Sustainable Energy*, **41(2)**: (2022).

[32] Corporation R.G., Product Specification List of Rubitherm Gmbh, 20.08.2019 [Cited 2019 20.08.2019]; Product Specification List of Rubitherm GmbH].

[33] Zarandi M.M., Analysis on Iranian Wind Catcher and its Effect on Natural Ventilation as a Solution Towards Sustainable Architecture (Case Study: Yazd), *Eng. Technol.*, **54**: 574-579 (2009).

[34] Patankar S., "Numerical Heat Transfer and Fluid Flow", CRC Press (2018).

[35] Stefanescu D.M., "Science and Engineering of Casting Solidification", Springer (2015).

[36] Yang H., He Y., Solving Heat Transfer Problems with Phase Change Via Smoothed Effective Heat Capacity and Element-Free Galerkin Methods, *International Communications in Heat and Mass Transfer*, **37(4)**: 385-392 (2010).

[37] Kuznik F., Virgone J., Roux J.-J., Energetic Efficiency of Room Wall Containing PCM Wallboard: A Full-Scale Experimental Investigation, *Energy and Buildings*, **40(2)**: 148-156 (2008).

[38] Charvát P., Klimeš L., Ostrý M., Numerical and Experimental Investigation of a PCM-Based Thermal Storage Unit for Solar Air Systems, *Energy and Buildings*, **68**: 488-497 (2014).